

## 4.2. X-RAYS

Table 4.2.1.6. Comparison of storage-ring synchrotron-radiation sources; the parameters were correct in 1985 and, for some sources, may be substantially different from those at earlier or later periods; after Buras &amp; Tazzari (1984), courtesy of ESRP

Storage ring	Source type	No. of poles	$I$ (mA)	$E$ (GeV)	$R$ (m)	$\sigma_x$ (mm)*	$\sigma_z$ (mm)*	$\sigma'_z$ (mrad)*	$\lambda_c$ (Å)	$E_c$ (keV)	Flux $\left[ \frac{\text{photons s}^{-1}}{\text{mrad} \times 0.1\% \text{ BW}} \right]$	
											at $\lambda_c$	at 1.54 Å
(1) ESRF	BM	–	100	5.0	20.0	0.092	0.100	0.008	0.9	14	$8 \times 10^{12}$	$1 \times 10^{13}$
(2) ESRF	W	30	100	5.0	11.56	0.062	0.040	0.016	0.5	24	$2.4 \times 10^{14}$	$3 \times 10^{14}$
(3) ADONE (Frascati)	BM	–	100	1.5	5.0	0.8	0.4	0.04	8.0	1.5	$2.4 \times 10^{12}$	$5 \times 10^{10}$
(4) ADONE (Frascati)	W	6	100	1.5	2.6	1.4	0.24	0.08	4.3	3	$1.4 \times 10^{13}$	$3.4 \times 10^{12}$
(5) SRS (Daresbury)	BM	–	300	2.0	5.56	2.7	0.23	0.05	4.0	3	$1 \times 10^{13}$	$3 \times 10^{12}$
(6) SRS (Daresbury)	W	1	300	2.0	1.33	5.3	0.17	0.05	0.9	13	$1 \times 10^{13}$	$1.2 \times 10^{13}$
(7) DCI (Orsay)	BM	–	250	1.8	3.82	2.72	1.06	0.06	3.6	3.4	$7 \times 10^{12}$	$2.4 \times 10^{12}$
(8) DORIS (Hamburg)	BM	–	100	3.7	12.22	1.0	0.3	0.05	1.3	9.2	$6 \times 10^{12}$	$6.4 \times 10^{12}$
(9) DORIS (Hamburg)	BM	–	40	5.0	12.22	1.3	0.65	0.065	0.55	23	$3 \times 10^{12}$	$4.4 \times 10^{13}$
(10) DORIS (Hamburg)	W	32	100	3.7	20.57	1.5	0.4	0.033	2.3	5.5	$1.9 \times 10^{14}$	$1.3 \times 10^{14}$
(11) CESR (Cornell)	BM	–	40	5.5	32.0	1.44	1.0	0.065	1.0	11.5	$3.5 \times 10^{12}$	$4 \times 10^{12}$
(12) CESR (Cornell)	W	6	40	5.5	13.2	1.9	1.2	0.05	0.4	28	$2 \times 10^{13}$	$3 \times 10^{13}$
(13) NSLS X-ray (Brookhaven)	BM	–	300	2.5	6.83	0.25	0.1	0.01	2.4	5	$1 \times 10^{13}$	$8 \times 10^{12}$
(14) SPEAR	BM	–	100	3.0	12.7	2.0	0.28	0.05	2.7	5	$5 \times 10^{12}$	$3 \times 10^{12}$
(15) SPEAR	W	8	100	3.0	5.57	3.2	0.15	0.03	1.0	10	$3.8 \times 10^{13}$	$4.5 \times 10^{13}$
(16) SPEAR	W	54	100	3.0	8.36	3.2	0.15	0.03	1.7	7	$2.6 \times 10^{14}$	$2.4 \times 10^{14}$
(17) Photon Factory (Tsukuba)	BM	–	150	2.5	8.66	2.2	0.6	0.14	3.0	4	$6 \times 10^{12}$	$3 \times 10^{12}$
(18) Photon Factory (Tsukuba)	W	3	150	2.5	1.85	1.9	0.7	0.18	0.7	19	$1.8 \times 10^{13}$	$2.5 \times 10^{13}$
(19) VEPP-3	BM	–	100	2.2	6.15	6.15	0.08	0.02	3.0	4	$3.5 \times 10^{12}$	$1.5 \times 10^{12}$

\* One standard deviation of Gaussian distribution.

with a frequency conversion system that shifts the peak power of the laser light from the infrared (1.054  $\mu\text{m}$ ) to the ultraviolet (0.351  $\mu\text{m}$ ) (Seka, Soures, Lund & Craxton, 1981). This led to a more efficient X-ray production, which permitted a more than twofold increase in X-ray flux, even though the maximum pulse energies had to be reduced to  $\sim 50$  J to prevent damage to the optical components (Yaakobi, Boehli, Bourke, Conturie, Craxton, Delettretz, Forsyth, Frankel, Goldman, McCrory, Richardson, Seka, Shvarts & Soures, 1981). Forsyth & Frankel (1984) used the plasma X-ray source for diffraction studies with 4.45 Å X-rays with a focusing collimation system that delivered up to  $10^{10}$  photons pulse $^{-1}$  to the specimen over an area approximately 150  $\mu\text{m}$  in diameter. More recently, by special target design (Forsyth, 1986, unpublished), fluxes have been increased by factors of 2 to 3 without altering the laser output. Other plasma sources have been described by Collins, Davanloo & Bowen (1986) and by Rudakov, Baigarin, Kalimin, Korolev & Kumachov (1991).

The cost of plasma sources is about an order of magnitude greater than that of rotating-anode generators (Nagel, 1980). Their use is at present confined to flash-diffraction experiments, since the duty cycle is a maximum of one flash every 30 min. Attempts are being made to increase the laser repetition rate; a

substantial improvement could lead to a source that would rival storage-ring sources.

## 4.2.1.7. Other sources of X-rays

Parametric X-ray generation can be described as the diffraction of virtual photons associated with the field of a relativistic charged particle passing through a crystal. These diffracted photons appear as real photons with an energy that satisfies Bragg's law for the reflecting crystal planes, so that the energy can be tuned between 5 and 45 keV by rotating the mosaic graphite crystal. Linear accelerators with an energy between 100 and 500 MeV produce the incident relativistic electron beam (Maruyama, Di Nova, Snyder, Piestrup, Li, Fiorito & Rule, 1993; Fiorito, Rule, Piestrup, Li, Ho & Maruyama, 1993).

Transition-radiation X-rays with peak energies between 10 and 30 keV are produced when electrons from 100 to 400 MeV strike a stack of thin foils (Piestrup, Moran, Boyers, Pincus, Kephart, Gearhart & Maruyama, 1991). Quasi-monochromatic X-rays result from a selection of target foils with appropriate  $K$ -,  $L$ - or  $M$ -edge frequencies (Piestrup, Boyers, Pincus, Harris, Maruyama, Bergstrom, Caplan, Silzer & Skopic, 1991).

#### 4. PRODUCTION AND PROPERTIES OF RADIATIONS

Table 4.2.1.7. Intensity gain with storage rings over conventional sources; from Farge & Duke (1979), courtesy of ESF

	GX6 rotating-anode tube 2.4 kW (Cu $K\alpha$ emission)	DCI 1.72 GeV and 240 mA	ESRF 5 GeV and 565 mA
Brightness impact ↑			
Small-angle scattering with a double monochromator		×500 to 1000	×15000 to 3000
Protein crystallography with a single-focus monochromator 1 mm <sup>3</sup> samples Small samples		×50 to 160 ×30 to 60	×900 to 1800 ×650 to 1300
Diffuse scattering (wide angles, low resolution and large samples) with a curved graphite monochromator		×20 to 40	×160 to 320
Non characteristic wavelength (continuous background) EXAFS experimental set-up with a 100 kW rotating anode		×10 <sup>4</sup>	×10 <sup>5</sup>

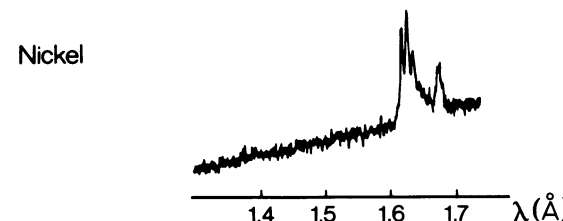
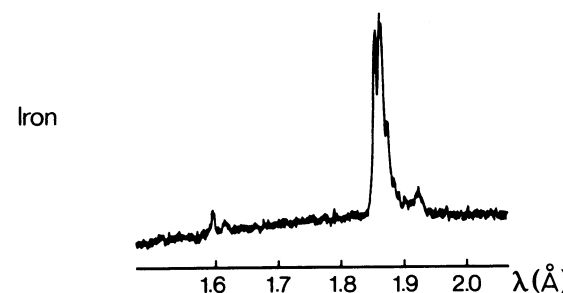
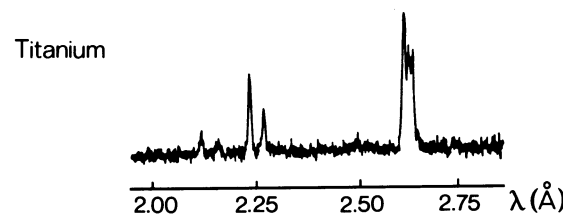
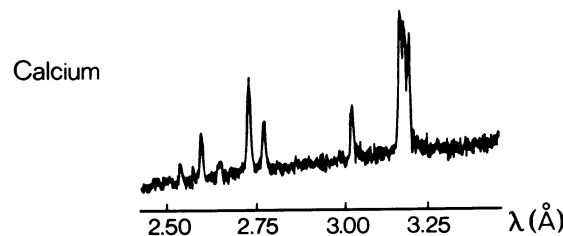
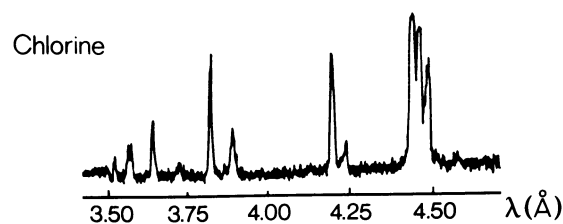


Fig. 4.2.1.12. X-ray emission from various laser-produced plasmas. From Forsyth & Frankel (1980); courtesy of J. M. Forsyth.

Channelling radiation, resulting from the incidence of electrons with an energy of only about 5 MeV on appropriately aligned diamond or silicon crystals hold out the hope of producing a bright tunable X-ray source.

One or more of these methods may, in the future, be developed as X-ray sources that can compete with synchrotron-radiation sources.

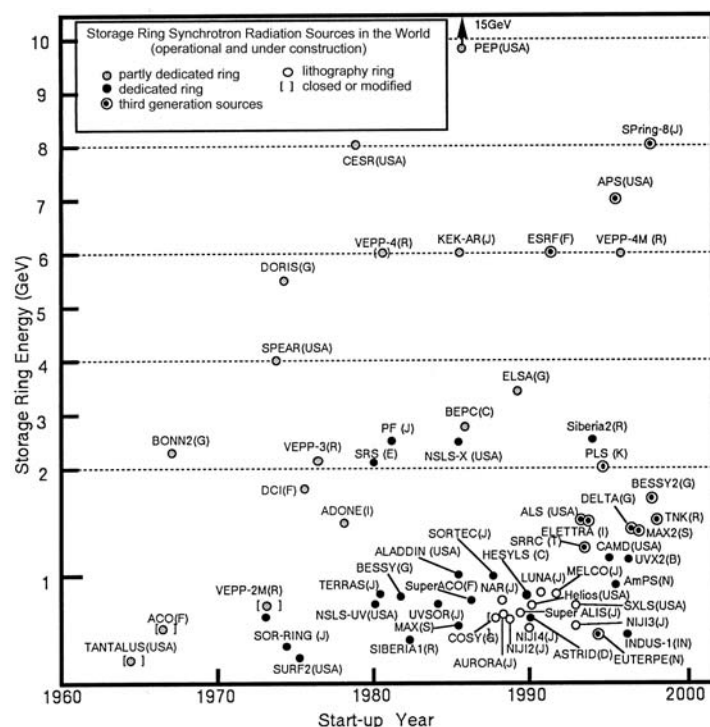


Fig. 4.2.1.11. The evolution of storage-ring synchrotron-radiation sources over the decades, as illustrated by their increasing number and range of machine energies (based on Suller, 1992).